Making the Diagnosis of Myositis: Muscle MRI

16

Jonas Lötscher, Balazs K. Kovacs, and Ulrich A. Walker

Introduction

Myositis patients present with acute or subacute muscle weakness, typically affecting the proximal muscles of the upper extremity, lower extremity, and spine in a symmetric distribution. Five main clinico-pathological subtypes are distinguished among adult patients, including dermatomyositis (DM), cancer-associated myositis (CAM), polymyositis (PM), immune-mediated necrotizing myopathy (IMNM), sporadic inclusion-body myositis (sIBM), and overlap myositis (or myositis associated with other systemic autoimmune rheumatic diseases) [1].

The diagnosis of a myositis patient includes the typical presentation of symmetric proximal muscle weakness, elevated muscle enzymes (e.g., creatine kinase or CK), a myopathic electromyographic (EMG) pattern, characteristic pathological changes in skeletal muscle biopsy, and the presence of myositis-specific autoantibodies. A critical step in the diagnosis of myositis is to exclude myositis mimics, especially in the setting of "polymyositis" where the pathognomonic rash of DM is lacking and the observation that many mimics such as

Table 16.1 Potential roles of muscle imaging in IIM

Sensitive detection of muscle pathology
Exclusion of IIM mimics
Differentiation of IIM subsets
Guiding muscle biopsy
Disease activity vs. damage
Response to therapy

metabolic myopathies and muscular dystrophies [2] may present with the aforementioned features. MRI could aid in recognizing patterns of muscle involvement among various mimics and myositis subtypes. Although EMG is used as a guide to muscle biopsy, MRI may provide an improved and noninvasive tool for selecting the site of muscle biopsy. Despite advancement in the outcome measures of myositis, we currently lack an objective imaging measure to gauge the response to therapy. Moreover, differentiating disease activity vs. damage, both of which lead to muscle weakness, poses a significant clinical challenge which may be addressed by muscle MRI. An early and accurate monitoring of disease activity is of great importance in the tailoring of treatment intensity. In this chapter, we review the different roles of MRI and other imaging tools assisting in the diagnosis and management of idiopathic inflammatory myopathies (IIM) (Table 16.1).

MRI Protocols in IIM

MRI provides an excellent soft-tissue contrast at high resolution. Further, general advantages

J. Lötscher · U. A. Walker (✉)
Department of Rheumatology, Unispital Basel, Basel, Switzerland
e-mail: jonas.loetscher@unibas.ch; ulrich.walker@usb.ch

B. K. Kovacs
Department of Radiology, Unispital Basel, Basel, Switzerland

of MRI are its noninvasiveness, broad availability, and lack of ionizing radiation. In contrast to ultrasound, MRI provides better resolution of the soft tissue and bone. Muscle abnormalities found by MRI in IIM include muscle edema, fatty replacement, and muscle atrophy. The sequences most commonly used (Table 16.2) in musculoskeletal MRI are T1-weighted (T1w),

Table 16.2 MRI sequences in myositis imaging. Examples are shown in Fig. 16.1

MRI sequences	Useful key features	Potential application
T1w	High anatomical resolution	Damage evaluation (atrophy, fibrosis, and fatty replacement)
Fat-suppressed T2w	Detection of muscle edema Resolution superior to fluid-sensitive sequences	Disease activity, target muscle biopsy, therapeutic response
Fluid-sensitive Sequences (STIR, TIRM, SPAIR)	Detection of muscle edema	Disease activity, target muscle biopsy, therapeutic response
Gadolinium	Contrast enhancement not superior to muscle edema seen on fluid-sensitive sequences	Not commonly used

Fig. 16.1 (**a**) MR sequences used in diagnosing myositis of a healthy patient. (**b**) Identical MR sequences in a 71-year-old male patient with sIBM. The TIRM and T2w fat-saturated images reveal muscle edema in the right tibial anterior muscle as hyperintensities (white arrow) and enhancement (black arrow with white edge). Fatty infiltration of the left tibial anterior muscle is revealed as hyperintensity in T1w images (gray arrow)
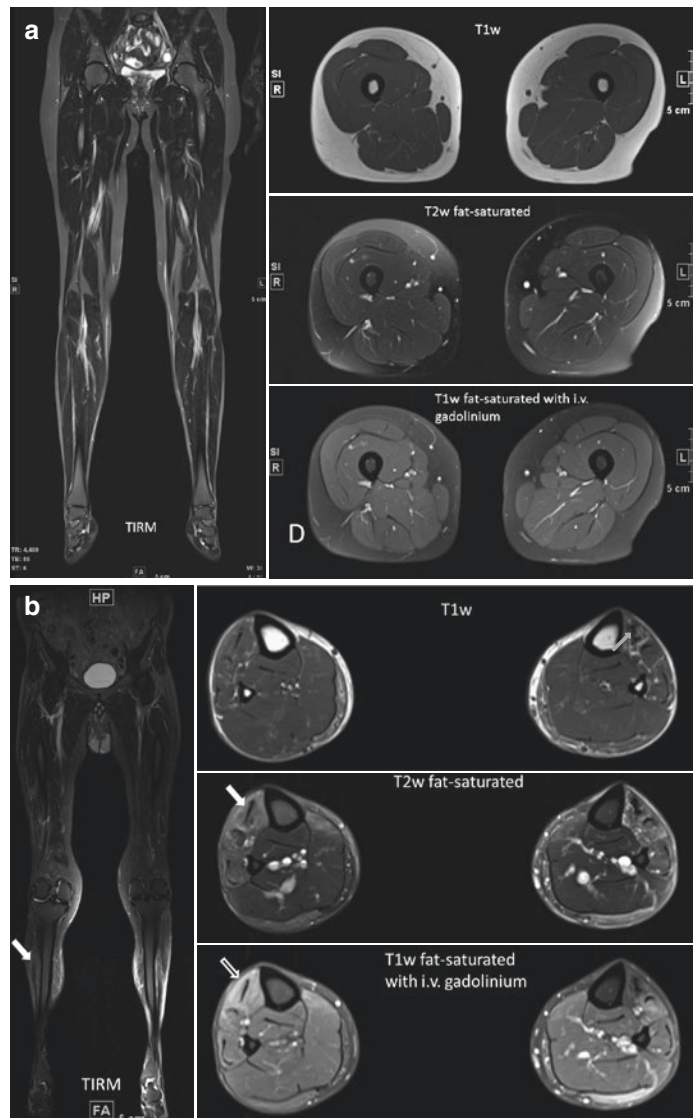
T2-weighted (T2w), both with and/or without fat signal suppression, and fluid-sensitive sequences (e.g., short tau inversion recovery (STIR), turbo inversion recovery magnitude (TIRM), spectral attenuated inversion recovery (SPAIR)) [3]. T1w images provide high anatomical resolution and are sensitive in detecting fat but insensitive with regard to water detection. The signal intensity of healthy muscle in T1w sequences is below water and above fat. T1w sequences are used to depict fatty atrophy and to discriminate between acute and chronic diseases.

In T2w sequences both water and fat appear hyperintense, and the signal intensity of normal muscle is lower than water and fat. Muscle edema reflects an increased amount of intracellular or extracellular free water [4] and thus appears hyperintense in the fluid-sensitive T2w sequences. Since fat also appears hyperintense in T2w sequences, fat-suppressed T2w sequences have been developed, facilitating the specific detection of edema.

STIR, TIRM, and SPAIR sequences are fluid-sensitive sequences that use different techniques to better detect water. In muscle protocols they are used to sensitively reveal muscle edema.

In the more acute phases of IIM, the signal intensity of such fluid-sensitive sequences correlates with disease activity [5].

Gadolinium contrast does not enhance the detection of muscle edema by fluid-sensitive sequences and is also not superior to T2w fat-suppressed sequences. Since the application of gadolinium also requires longer scan times, muscle MRI is usually performed without contrast agents [3, 6].

Types of Muscle Magnetic Resonance Imagings

(a) *Thigh Muscle MRI:* For practical reasons, the thighs are often selected for MRI, as proximal leg muscles are frequently involved in myositis and a convenient target for biopsy
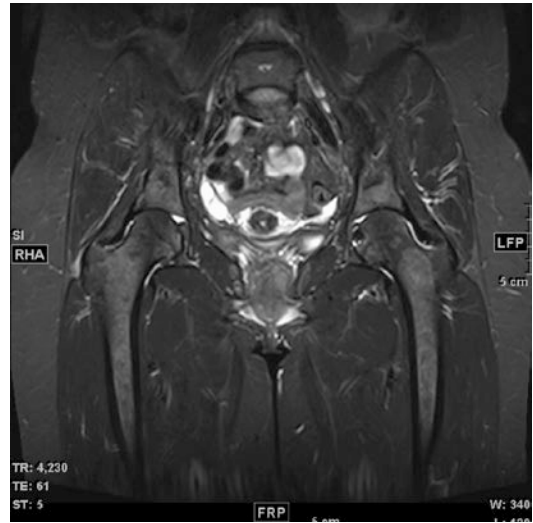

Fig. 16.2 Thigh muscle MRI—coronal TIRM image in a healthy female person

[7]. The scan time of such regional MRI is relatively short, but at the same time muscle involvement in other body regions remains undetected (Fig. 16.2).

(b) *Whole-Body Magnetic Resonance Imaging:* Whole-body MRI (wb-MRI) allows a comprehensive visualization of all large muscle groups, rendering it especially useful in early disease stages when some muscles may only be involved subclinically [8, 9]. Furthermore, wb-MRI may reveal characteristic distribution patterns of muscle inflammation assisting in the differential diagnoses. In the case of paraneoplastic IIM, wb-MRI also offers the possibility of detecting the underlying malignancy. The duration of the standard wb-MRI protocol is 45 minutes, which may be challenging for the patient and clinical centers in terms of time and cost-effectiveness (Fig. 16.3).

(c) *Short Whole-Body Magnetic Resonance Imaging:* A shortened wb-MRI protocol with omission of the trunk has recently been reported. The diagnostic accuracy of this shortened protocol was similar to the regular wb-MRI protocol with a 30% time-saving [10].

Fig. 16.3 Coronal TIRM image of a whole-body MRI in a healthy female
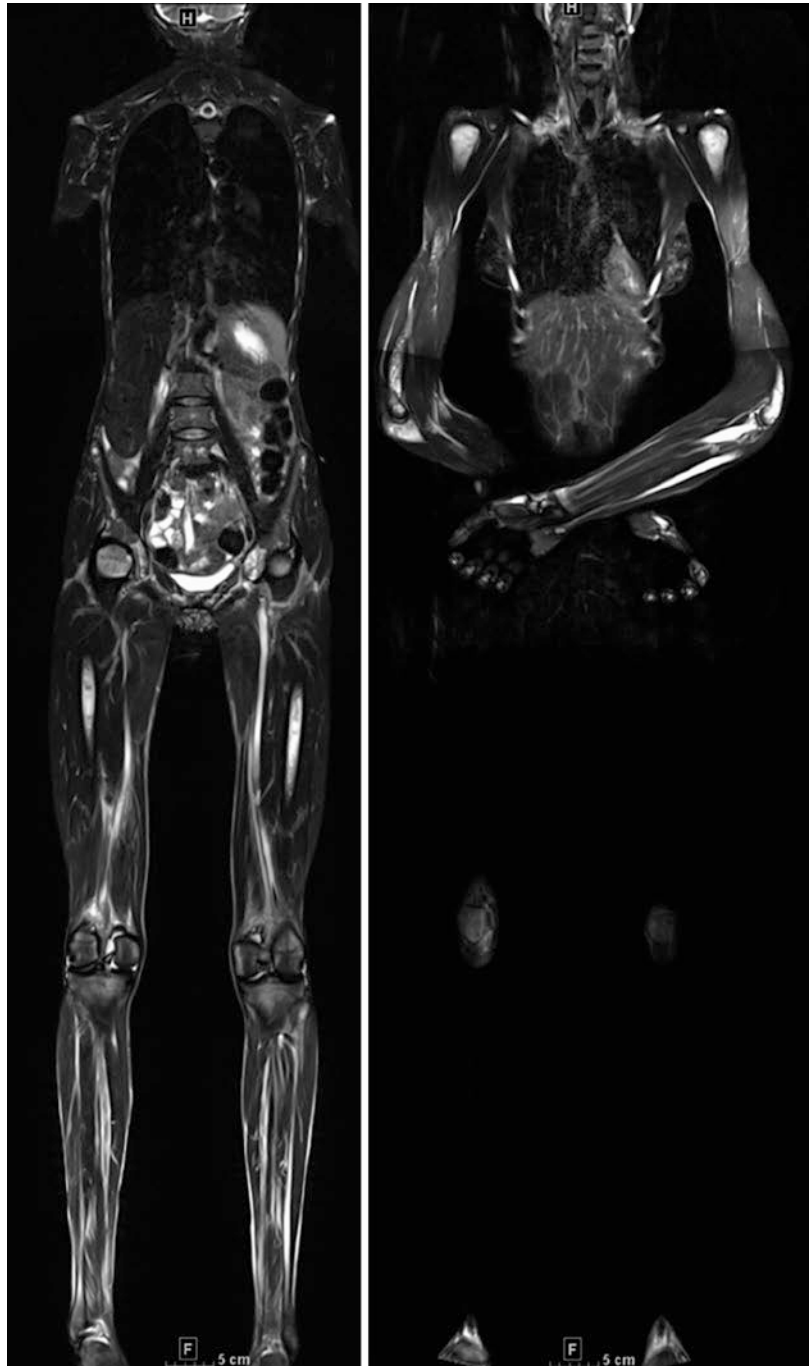
Diagnostic Yield of Magnetic Resonance Imaging

In some centers muscle MRI of the proximal extremities is routinely performed in the diagnos-tic workup of IIM. In the vast majority of patients with acute IIM (76–97%), MRI shows muscle edema, consistent with inflammation [11]. This finding is significantly associated with muscle weakness and elevated serum CK values [5, 12],

Table 16.3 Diagnostic yield of thigh MRI [15]

Type of myositis	Sensitivity	Specificity
PM	63.1%	59.0%
DM	82.6%	64.2%
IMNM	62.4%	90.8%
IBM	83.7%	87.7

while fatty infiltration and muscle atrophy represent chronic myositis.

A retrospective study evaluated the diagnostic yield of MRI in comparison with the clinical diagnosis of myositis in 51 IIM patients (29 PM/22 DM) [12]. In this study, MRI had a sensitivity of 92.3% and a specificity of 83.3% for PM/DM. A similar sensitivity of 91% was reported in a prospective study of 48 patients with suspected IIM (DM, PM, IMNM, nonspecific myositis), but a lower specificity of 61%, when biopsy-proven myositis was the gold standard [13]. There was no subgroup analysis done to differentiate sensitivity and specificity for PM, DM, or IMNM or nonspecific myositis. In a retrospective evaluation of 17 patients with sIBM, a characteristic pattern of muscle involvement was defined [14]. Compared to MRI findings of 118 patients with other myopathies, the authors reported a sensitivity and specificity, both exceeding 95%. The pattern of muscle involvement characteristic for sIBM is described in more detail below. One study [15] examined the specificity and sensitivity of thigh MRI in the detection of IIM subtypes (Table 16.3).

Distribution of Magnetic Resonance Imaging Involvement in IIM Subtypes

Several studies have demonstrated that the IIM subtypes tend to affect particular muscle groups. The recognition of such different patterns may help to narrow the differential diagnosis.

In the early course of PM, for example, the muscle edema is distributed symmetrically in the proximal muscles of all extremities. Muscle involvement of the upper extremities may include the deltoid, trapezius, biceps, and triceps muscle [8, 16]. In the lower extremities, the quadriceps
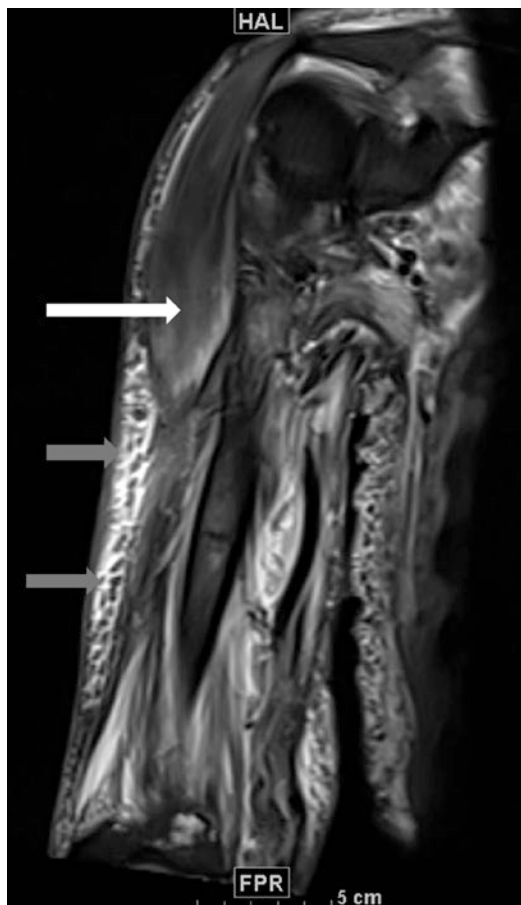

Fig. 16.4 TIRM sequence of a 63-year-old male patient with extensive intramuscular (white arrow) and subcutaneous edema (gray arrow)

muscles (vastus medialis, intermedius, and lateralis) and the tibialis anterior are preferentially involved [17]. In progressive disease, an involvement of pharyngeal muscles and neck flexors has also been observed [18].

In DM, the MRI pattern is similar to PM in its symmetry and involvement of proximal muscle groups (Fig. 16.4). However, edematous inflammation of muscle fasciae (50–100%) [19] and subcutaneous fatty tissue (85%) [20] are also common (Figs. 16.4 and 16.5). Five of 26 prospectively studied juvenile DM patients with subcutaneous edema on the initial thigh MRI developed clinically apparent calcinosis at the same location within 9 months [20]. Patients with a more diffuse or homogenous distribution of

Fig. 16.5 Coronal TIRM image of the shoulder girdle (**a**) and thighs (**b**) in a 66-year-old male patient with DM demonstrating extensive edema in all proximal muscles
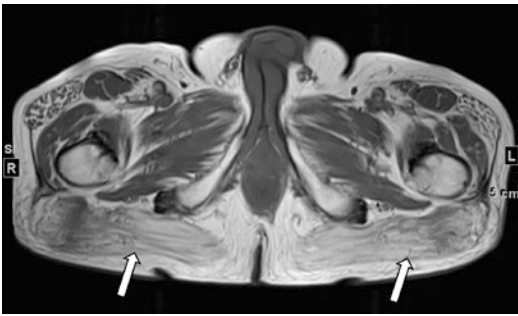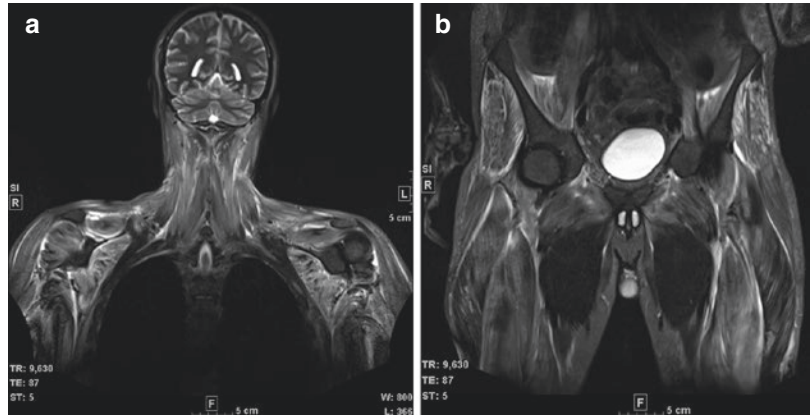

Fig. 16.6 T1-weighted axial image of the pelvis of an 80-year-old male patient with IMNM. The arrows show the greater gluteal muscles with excessive fat degeneration

muscle inflammation had a more severe disease course compared to patients with a more patchy distribution [21].

In IMNM, MRI revealed characteristic edematous and atrophic changes of the hip rotators and glutei (Fig. 16.6) [15]. Muscle abnormalities in IMNN [associated with antibodies directed against signal recognition particle (SRP) or HMG-CoA reductase (HMGCR); see Chap. 24] appeared to be more severe compared to patients with DM or PM [15]. On thigh MRI, patients with anti-SRP antibodies had more atrophy and fatty replacement than patients with anti-HMGCR antibodies [15]. However, there are no studies to differentiate IMNM from PM findings on MRI.

In sIBM, fatty infiltration and atrophy are more common than inflammatory changes. In comparison to PM, the lesions of sIBM tend to be more

asymmetric and distal in location [6]. In the thigh muscles, a predominant involvement of the quadriceps with relative sparing of the rectus femoris is reported [22, 23]. Some authors describe a "melted" appearance of the distal quadriceps and involvement of the sartorius muscle [14]. In the calves, the medial gastrocnemius is most frequently infiltrated with fat, whereas the soleus muscle is relatively spared (Fig. 16.7). Corresponding to the weakness of finger flexors, MRI may reveal an intramuscular fat accumulation in the flexor digitorum profundus muscles [22, 23].

Magnetic Resonance Imaging in Guiding Muscle Biopsies

MRI represents a sensitive tool to detect muscle involvement in suspected IIM, but the detection of muscle edema and fatty atrophy by MRI is not specific for inflammation. Thus, the diagnosis of IIM should never be based on MRI alone and a muscle biopsy is often required for confirmation [2].

The regional distribution of muscle involvement in IIM may range from a few muscles to several muscle groups, but the disease process may be patchy (Fig. 16.8). Although EMG-guided biopsy has a high yield, it is invasive and painful, suggesting the need for an imaging-guided approach. Moreover, the "blind" acquisition of a muscle biopsy is error-prone, as indicated by a retrospective study of 153 PM/DM patients in which 25% of blind

Fig. 16.7 Seventy-one-year-old male patient with sIBM. Axial T1w, fat-saturated T2w, and fat-saturated T1w images after contrast administration at identical levels demonstrating symmetric fatty infiltration of the medial head of the gastrocnemius (broad white arrow). There is some edema and gadolinium enhancement (asterisks) in the right tibialis anterior muscle (thin white arrow) and in the lateral head of the left gastrocnemius (thin gray arrow)
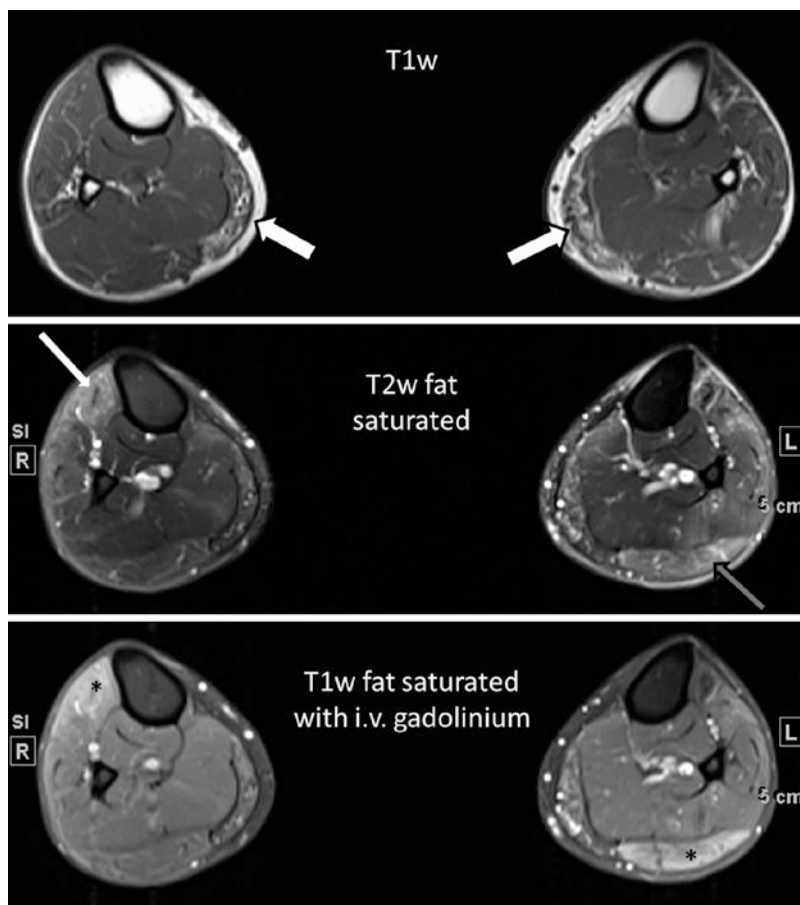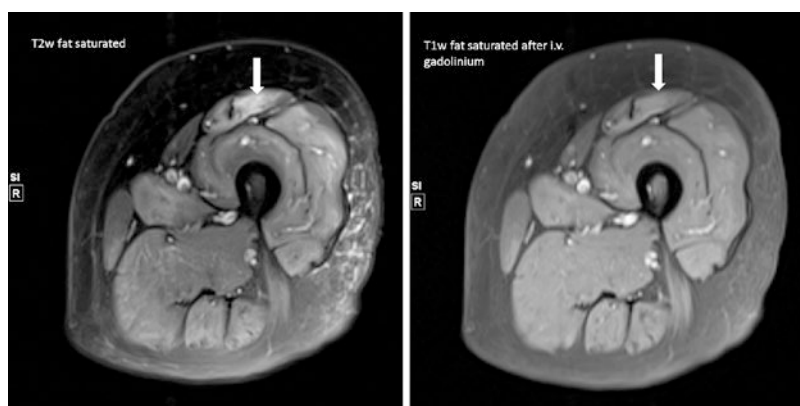

Fig. 16.8 Eighty-year-old female patient with edema and contrast enhancement restricted to the rectus femoris muscle and almost complete sparing of the vastus lateralis and medialis muscles. The rectus femoris was chosen for biopsy, yielding IMNM

biopsies lacked inflammatory infiltrates [24]. Muscle biopsies from sites that featured signal hyperintensity in T2w fat-suppressed and STIR images contained significantly more inflammatory cells than those obtained from sites with a normal MRI [5]. In a prospective study of 48 patients with suspected IIM, the overall false-negative rate of muscle biopsy was 23% [13]. Biopsies, which were performed at sites of high signal intensity in T2w fat-suppressed or

STIR images revealed a false-negative rate of 19%, compared with 67% of biopsies at MRI-negative sites [13]. Additional work suggests that a pre-biopsy MRI is cost-effective due to lower re-biopsy rates [25]. Thus, the use of MRI in guiding muscle biopsy increases the diagnostic accuracy and MRI may replace an EMG-guided approach in the future regarding the workup of myositis.

MRI Pattern in Myositis Mimics

Although muscle edema and fatty atrophy are not observed in normal muscle and can be detected sensitively by MRI, they are not specific for IIM (Fig. 16.9a, b). The differential diagnosis of IIM is wide and includes inherited myopathies (muscle dystrophies and metabolic myopathies), as well as myopathies due to medications, infections, or endocrine disorders. The MRI presentation of the IIM mimics can be similar to the involvement seen in true idiopathic inflammation, although a few IIM mimics have more specific radiographic features (Table 16.4).

Muscle edema can also be seen in numerous other conditions such as after radiation therapy and muscle injury [26], rhabdomyolysis [27], and even after physical exercise [28]. Fatty atrophy is also observed after muscle denervation [29] and in chronic disuse states [30].

Magnetic Resonance Imaging for Disease Activity Versus Damage

The noninvasive nature and lack of ionizing radiation render muscle MRI suitable for serial use in the longitudinal monitoring of disease activity and damage. It may be clinically difficult to differentiate ongoing myositis activity in patients with persistent or recurrent muscle weakness from irreversible damage or glucocorticoid myopathy. Similarly, the determination of serum muscle enzymes may be of limited value in patients (where the CK can be normal in the presence of active disease) as well as in long-standing
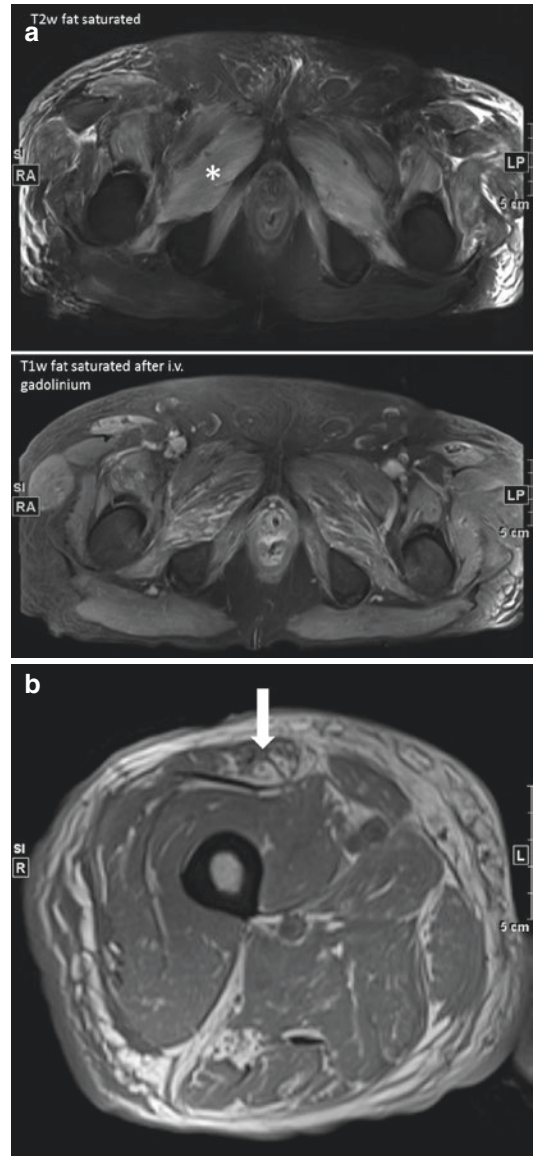
Fig. 16.9 (**a**) Muscle edema in a 75-year-old male with limb-girdle muscle dystrophy type 2a (calpainopathy). Extensive edema in most pelvic muscles, predominantly in the external obturator muscle (asterisk) with slight linear and not patchy contrast enhancement. (**b**) Fatty infiltration of the right rectus femoris muscle (arrow) in the same patient

myopathies. In this situation, the detection of muscle edema by MRI may help to distinguish between acute inflammation and chronic muscle damage (Fig. 16.10 top row) [31], providing an important clue for therapeutic decision-making.

**Table 16.4** Clinical presentation and MRI findings of select IIM mimics

IIM mimic	Clinical presentation	MRI findings	Ref
Limb girdle dystrophy (LGMD) 2A	Onset up to eighth decade. Slowly progressive weakness and atrophy of proximal muscles due to mutations in *dysferlin* gene. Autosomal recessive inheritance. Endomysial or perivascular T lymphocytes possible	Predominant atrophy of posterior thigh muscles (semimembranosus, semitendinosus, biceps femoris, and adductors). At calf levels, soleus muscle and the medial head of the gastrocnemius involved, sparing of the lateral gastrocnemius	[64]
Becker's muscular dystrophy	X-chromosomal recessively inherited mutations in the *dystrophin* gene. Progressive weakness of legs and pelvic muscles. Calf hypertrophy. Cardiomyopathy	Prominent involvement of the gluteus maximus (80% of patients), atrophy of gluteus medius, adductor magnus, long head of biceps femoris, and semimembranosus (70% each)	[65]
Statin-induced myopathy	Can range from myalgia to rhabdomyolysis	Fatty atrophy in T1w sequences (29% of patients). Edema in 62% of T2w STIR images, mainly in dorsal thigh muscles (biceps femoris, semimembranosus, semitendinosus) and superficial calf muscles (soleus and gastrocnemius). Muscle edema associated with elevated serum CK and weakness	[66]
Infectious myositis	Viral, bacterial, fungal or parasitic. Bacterial and fungal myositis tends to present as a localized myositis, and viral and parasitic muscle infections tend to present as diffuse myositis. Pyomyositis due to *staphylococcus aureus*, predominantly in the tropics. Polymyositis in early HIV infection, possibly T-cell-mediated. Bilateral proximal muscle weakness and CK elevation	In pyomyositis abscess formations are hypointense in T1w and hyperintense in T2w and STIR sequences with a hyperintense rim on unenhanced T1w images and peripheral enhancement after contrast medium application. In myositis due to *Candida tropicalis*, MRI showed numerous microabscesses and diffuse muscle edema. Pork tapeworm causes cystic lesions with low signal in T1w and high signal in T2w images. MRI may depict scolices. HIV-associated polymyositis may show abnormal signal intensity in T2w and STIR sequences	[67–74]
Diabetic muscle infarction	Rare complication of poorly controlled insulin-dependent diabetes. Pain and swelling, mainly of thighs and calves	Diffuse edematous enlargement of involved muscles and increased signal intensity on T2w, STIR, and gadolinium-enhanced images	[75, 76].
Rhabdomyolysis	Life-threatening from a large variety of causes, including drug abuse, excessive muscle exercise, ischemic injury, infections, or direct muscle injury	Widespread muscle edema. Affected muscles hyperintense in T2w and STIR sequences and hypointense in T1w	[77, 78]
Sarcoidosis	Four types of muscle involvement. Acute myositis: painful swelling of muscles. Chronic myopathy: muscle weakness and atrophy. Nodular type: palpable intramuscular masses. Asymptomatic type: Incidental detection of granulomas in biopsy	Acute sarcoid myositis: diffusely increased signal in T2w sequences. Asymptomatic and chronic myopathy: The granulomas along muscle fibers cannot be detected by MRI, only by histology. Nodular sarcoidosis: more specific with a star-shaped central decrease of signal intensity in axial T1w and T2w sequences, surrounded by increased intensity ("dark-star" sign). Axial or sagittal images, in which muscle fibers run parallel, show three stripes: The inner stripe with decreased signal intensity and two outer stripes with increased signal intensity ("three stripes"-sign). On histology the central area with decreased signal intensity is fibrotic, and the surrounding hyperintensity represents granulomatous inflammation	[79–83]

Table 16.4 (continued)

IIM mimic	Clinical presentation	MRI findings	Ref
Hypothyroid myopathy	Muscle stiffness and hypertrophy in untreated hypothyroidism	Distal legs predominantly affected. Hypertrophic muscles on T1w, increased signal intensity on T2w and STIR images	[84–86]
Metabolic myopathies	Exercise intolerance and recurrent rhabdomyolysis	Lower body MRI of 20 patients with long-chain fatty acid oxidation disorders demonstrated distinct patterns of increased signal intensity in T1W and STIR sequences. In very long-chain acyl-CoA dehydrogenase deficiency (VLCADD), increased T1W signals in proximal muscles. In long-chain hydroxyacyl-CoA dehydrogenase deficiency (LCHADD), mainly distal involvement. STIR hyperintensity in VLCADD and LCHADD associated with increased serum CK T1w changes reflect fatty infiltration, STIR hyperintensity edema	[87]

Fig. 16.10 Focal active inflammation in the vastus medialis muscle of a 79-year-old male with IMNM (upper row, white arrows). Extensive fatty infiltration of greater gluteal muscle (lower row, gray arrows)

## Magnetic Resonance Imaging for Treatment Response
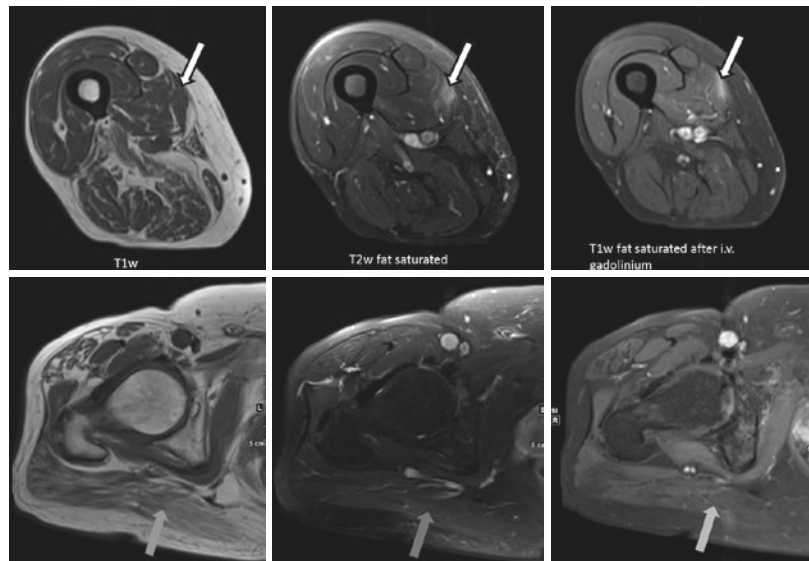
Muscle weakness in the setting of MRI findings of extensive replacement by fatty tissue (Fig. 16.9 bottom row) has been correlated with a lack of improvement with immunosuppressive therapy [32].

Several studies have shown that muscle edema on MRI decreases during therapy (Fig. 16.11) [5, 21, 33, 34]. Muscle MRI may even better reflect clinical improvement than muscle biopsy [5]. The presence of muscle edema on MRI is also significantly associated with the presence of muscle weakness and elevated serum CK values [5, 12]. In a study of 41 juvenile DM patients, 18 patients underwent a follow-up wb-MRI [21]. Eleven of these patients had lower MRI scores in response to treatment. Moreover, nine patients showed total resolution of inflammation in wb-MRI, whereas in the clinical assessment, only five patients met the criteria for remission. The authors suggest that loss of muscle strength may result from muscle damage rather than from

Fig. 16.11 Sequential images of a 22-year-old male with PM demonstrating regressing muscle edema (white arrows) and contrast enhancement (gray arrows) in the left lateral vastus muscle 5 months after the initiation of therapy
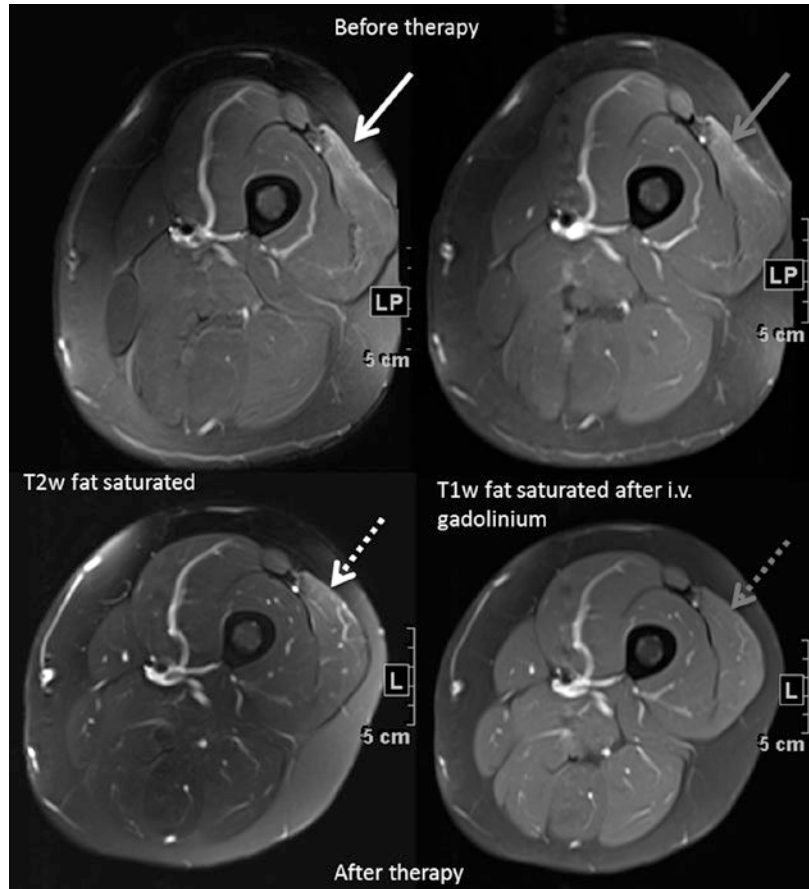
myositis activity, and that the clinical assessment has overestimated disease activity.

Taken together, these observations suggest that MRI provides valuable information regarding disease activity and treatment response. MRI may therefore complement the purely clinical assessment and serve as a myositis outcome measure. The IMACS group has now adopted the finding of muscle atrophy assessed by radiographic methods in its myositis damage index [35].

Other Advantages of Magnetic Resonance Imaging in Myositis

MRI can also be used to screen for cardiac involvement [36, 37] as heart-specific sequences (late contrast-enhanced T1w sequences) are added to the wb-MRI protocol. According to the Lake Louise consensus criteria, MRI findings are consistent with myocarditis if they meet at least two of the following three criteria: (1) increased signal intensity in T2w images representing edema, (2) increased early myocardial gadolinium enhancement reflecting hyperemia or capillary leakage, and (3) increased late gadolinium enhancement in a non-ischemic distribution representing irreversible cellular injury [38]. Left ventricular dysfunction and pericardial effusion may provide additional evidence for myocardial involvement. However, the performance of the myocarditis criteria has not been validated in IIM.

Finally, MRI may also detect intramuscular calcifications in IIM where fluid collections represent "milk of calcium." The latter have a variable signal amplitude on T2w images, depending on the calcium content of the collections [39].

Functional Magnetic Resonance Imaging Techniques

Blood oxygenation level-dependent MRI (BOLD MRI) is a functional MRI technique quantitating muscle microcirculation by measuring changes between diamagnetic oxy-hemoglobin and paramagnetic deoxy-hemoglobin. As the BOLD MRI signal depends mainly on blood oxygenation, blood flow can be derived under standardized conditions. In systemic sclerosis, BOLD MRI has revealed impaired skeletal muscle microcirculation [40]. BOLD MRI studies have not yet been carried out in IIM, but the technique has the capacity to noninvasively quantify vascular involvement in IIM, especially DM, where vasculopathy may be a key factor in pathogenesis.

Magnetic resonance spectroscopy (MRS) noninvasively quantifies pH and energy metabolites within tissues. In IIM, this technique has revealed impaired energy supply [41, 42] but is not part of the routine diagnostic armamentarium.

Diffusion-weighted (DWI) MRI is a functional MRI technique that measures the random motion of protons within water and calculates the extent of fluid motion in terms of diffusion and perfusion. IIM patients had increased diffusion values in inflamed muscles, whereas fatty-infiltrated muscles had decreased values [43].

T2 mapping is a different imaging method, which relies on proton transverse relaxation time (T2). T2 signals increase with augmented muscular water content, such as with edema or after exercise [44, 45]. The advantage of T2 mapping is that the technique provides a quantifiable measure of water content (and inflammation in myositis).

Muscle Ultrasound

The advantage of muscle ultrasound (US) over MRI consists of its broad availability, ease in handling, and lower cost. In the pediatric population, the use of muscle US is even more attractive as MRI often requires sedation in young children. A large study suggested that substitution of MRI for US in musculoskeletal diseases, when appropriate, could lead to several billion dollars of savings [46]. In this respect the use of US in diagnostic workup appears attractive.

In standard B-mode, normal muscle tissue has low echogenicity [47]. On longitudinal scans, the perimysium appears as oblique, parallel, echogenic striae against the hypoechoic background representing the muscle fibers [48]. On transverse scans, the perimysium appears as finely dotted echoes.

Conventional US has been evaluated in 61 patients with PM, DM, or sIBM. In acute DM/PM, capillary leakage blurs the normal muscle architecture and decreases echogenicity. The resulting edema can augment muscle volume. In chronic myositis, muscles become atrophic and infiltrated with fat and therefore have reduced volume and increased echogenicity [49]. Granulomatous myositis is characterized by the highest echo intensities and a tendency toward muscle hypertrophy [50].

The sensitivity of US in detecting muscle abnormalities of adult IIM patients was 83%, although statistically not superior to electromyography (92% sensitivity) and serum CK values (69% sensitivity) [50]. US offers the possibility to detect tissue calcifications as large hyperechoic foci with acoustic shadowing and fluid collections as "milk of calcium" [51, 52].

Contrast-enhanced power Doppler US was compared with MRI in a prospective study of 35 patients suspected to have DM or PM. The sensitivity of contrast-enhanced US was 73%, while the specificity was 91%. MRI however had nominally better figures (77% and 100%, respectively) [53]. Despite the inferiority compared to MRI, contrast-enhanced US may be an accessible and feasible alternative to MRI, especially in resource-poor settings. One of the major disadvantages of musculoskeletal US is that its performance is highly dependent on the experience of the examiner.

FDG-PET

Positron emission tomography (PET) uses short-lived positron-emitting radioisotopes as tracers. The uptake and storage of fluorine-18-labeled deoxyglucose (FDG) is routinely used for the

sensitive detection of lymphomas and other malignancies. Since inflammation increases the glucose demands of tissues, the diagnostic utility of FDG-PET is used in a variety of immune-mediated inflammatory conditions, such as sarcoidosis [54] and large-vessel vasculitis [55].

The role of FDG-PET in the diagnosis of IIM remains controversial. One study revealed an increased FDG-uptake in only 33% of IIM patients (13 PM/11 DM) [56], while a 12-patient (2 PM/10 DM) study showed a significantly increased FDG uptake in proximal muscles, but no significant correlations between uptake and disease duration, muscle strength, and CK levels [57]. A third study (5 PM/15 DM) noted a significant correlation between increased FDG uptake in proximal muscles and elevated CK values, decreased muscle strength, and inflammatory cell infiltrates in biopsy [58].

Since some IIM are associated with an increased risk of malignancy [59], FDG-PET may also provide a sensitive screening tool for neoplasm detection [60]. FDG-PET may also offer the added possibility to detect interstitial lung disease as an extramuscular complication [56, 58], but it is not yet part of the routine diagnostic workup of IIM.

^{99m}Technetium Pyrophosphate Scintigraphy

An increased uptake of ^{99m}technetium pyrophosphate (^{99m}Tc-PYP) in muscles affected by IIM has been described in case reports [61, 62]. A retrospective analysis of 166 patients with suspected myopathy assessed the diagnostic value of ^{99m}Tc-PYP scintigraphy [63]. The scan was positive in 60% of patients with the final diagnosis of IIM. ^{99m}Tc-PYP scintigraphy was however not able to discriminate between inflammatory and non-inflammatory myopathies. In individuals with biopsy-proven IIM, the diagnostic sensitivity was 43%, and its specificity was 60%. The low-positive and high-negative likelihood ratios of ^{99m}Tc-PYP muscle scintigraphy (5.0 and 0.65, respectively) suggest a limited value in the routine diagnostic workup of patients with suspected IIM.

Conclusion

MRI is perhaps the most valuable imaging technique in the diagnostic workup of IIM as it is sensitive, provides good spatial resolution, and resolves different muscle pathologies such as edema, fatty infiltration, atrophy, and concomitant fasciitis. Wb-MRI not only provides an overview of the extent of muscle involvement but may also reveal further organ pathology (heart involvement) and underlying malignancies.

IIM subgroups and IIM mimics may manifest with characteristic patterns of muscle involvement. Although MRI examination may therefore assist in narrowing down the differential diagnosis of a given myopathy, muscle biopsy still remains the gold standard for most myopathies. In this setting, MRI assists in the selection of a suitable biopsy site and lowers false-negative results compared with blind muscle biopsies.

Last but not least, muscle MRI can assist in the discrimination of active myosits and muscle damage and therefore may be a useful in assessing treatment response.

References

1. Dalakas MC, Hohlfeld R. Polymyositis and dermatomyositis. Lancet. 2003;362:971–82.
2. Lundberg IE, Miller FW, Tjarnlund A, et al. Diagnosis and classification of idiopathic inflammatory myopathies. J Intern Med. 2016;280:39–51.
3. Kuo GP, Carrino JA. Skeletal muscle imaging and inflammatory myopathies. Curr Opin Rheumatol. 2007;19:530–5.
4. Mattila KT, Lukka R, Hurme T, et al. Magnetic resonance imaging and magnetization transfer in experimental myonecrosis in the rat. Magn Reson Med. 1995;33:185–92.
5. Tomasova Studynkova J, Charvat F, Jarosova K, et al. The role of MRI in the assessment of polymyositis and dermatomyositis. Rheumatology. 2007;46:1174–9.
6. Dion E, Cherin P, Payan C, et al. Magnetic resonance imaging criteria for distinguishing between inclusion body myositis and polymyositis. J Rheumatol. 2002;29:1897–906.
7. Del GF, Carrino JA, Del GM, et al. Magnetic resonance imaging of inflammatory myopathies. Top Magn Reson Imaging. 2011;22:39–43.
8. O'Connell MJ, Powell T, Brennan D, et al. Whole-body MR imaging in the diagnosis of polymyositis. AJR Am J Roentgenol. 2002;179:967–71.

9. Cantwell C, Ryan M, O'Connell M, et al. A comparison of inflammatory myopathies at whole-body turbo STIR MRI. Clin Radiol. 2005;60:261–7.

10. Filli L, Maurer B, Manoliu A, et al. Whole-body MRI in adult inflammatory myopathies: do we need imaging of the trunk? Eur Radiol. 2015;25:3499–507.

11. Maurer B, Walker UA. Role of MRI in diagnosis and management of idiopathic inflammatory myopathies. Curr Rheumatol Rep. 2015;17:67.

12. Barsotti S, Zampa V, Talarico R, et al. Thigh magnetic resonance imaging for the evaluation of disease activity in patients with idiopathic inflammatory myopathies followed in a single center. Muscle Nerve. 2016;54:666–72.

13. van de Vlekkert J, Maas M, Hoogendijk JE, et al. Combining MRI and muscle biopsy improves diagnostic accuracy in subacute-onset idiopathic inflammatory myopathy. Muscle Nerve. 2015;51:253–8.

14. Tasca G, Monforte M, De FC, et al. Magnetic resonance imaging pattern recognition in sporadic inclusion-body myositis. Muscle Nerve. 2015;52:956–62.

15. Pinal-Fernandez I, Casal-Dominguez M, Carrino JA, et al. Thigh muscle MRI in immune-mediated necrotising myopathy: extensive oedema, early muscle damage and role of anti-SRP autoantibodies as a marker of severity. Ann Rheum Dis. 2017;76:681–7.

16. Khadilkar SV, Gupta N, Yadav RS. Cervicobrachial polymyositis. J Clin Neuromuscul Dis. 2014;16:59–68.

17. Reimers CD, Schedel H, Fleckenstein JL, et al. Magnetic resonance imaging of skeletal muscles in idiopathic inflammatory myopathies of adults. J Neurol. 1994;241:306–14.

18. Bohan A, Peter JB. Polymyositis and dermatomyositis (first of two parts). N Engl J Med. 1975;292:344–7.

19. Yoshida K, Kurosaka D, Joh K, et al. Fasciitis as a common lesion of dermatomyositis, demonstrated early after disease onset by en bloc biopsy combined with magnetic resonance imaging. Arthritis Rheum. 2010;62:3751–9.

20. Kimball AB, Summers RM, Turner M, et al. Magnetic resonance imaging detection of occult skin and subcutaneous abnormalities in juvenile dermatomyositis. Implications for diagnosis and therapy. Arthritis Rheum. 2000;43:1866–73.

21. Malattia C, Damasio MB, Madeo A, et al. Whole-body MRI in the assessment of disease activity in juvenile dermatomyositis. Ann Rheum Dis. 2014;73:1083–90.

22. Phillips BA, Cala LA, Thickbroom GW, et al. Patterns of muscle involvement in inclusion body myositis: clinical and magnetic resonance imaging study. Muscle Nerve. 2001;24:1526–34.

23. Cox FM, Reijnierse M, van Rijswijk CS, et al. Magnetic resonance imaging of skeletal muscles in sporadic inclusion body myositis. Rheumatology. 2011;50:1153–61.

24. Bohan A, Peter JB, Bowman RL, et al. Computer-assisted analysis of 153 patients with polymyositis and dermatomyositis. Medicine. 1977;56:255–86.

25. Schweitzer ME, Fort J. Cost-effectiveness of MR imaging in evaluating polymyositis. AJR Am J Roentgenol. 1995;165:1469–71.

26. Connell DA, Schneider-Kolsky ME, Hoving JL, et al. Longitudinal study comparing sonographic and MRI assessments of acute and healing hamstring injuries. AJR Am J Roentgenol. 2004;183:975–84.

27. Lu CH, Tsang YM, Yu CW, et al. Rhabdomyolysis: magnetic resonance imaging and computed tomography findings. J Comput Assist Tomogr. 2007;31:368–74.

28. Fleckenstein JL, Canby RC, Parkey RW, et al. Acute effects of exercise on MR imaging of skeletal muscle in normal volunteers. AJR Am J Roentgenol. 1988;151:231–7.

29. Fleckenstein JL, Watumull D, Conner KE, et al. Denervated human skeletal muscle: MR imaging evaluation. Radiology. 1993;187:213–8.

30. May DA, Disler DG, Jones EA, et al. Abnormal signal intensity in skeletal muscle at MR imaging: patterns, pearls, and pitfalls. Radiographics. 2000;20. Spec No:S295–315.

31. Rider LG, Werth VP, Huber AM, et al. Measures of adult and juvenile dermatomyositis, polymyositis, and inclusion body myositis: Physician and Patient/Parent Global Activity, Manual Muscle Testing (MMT), Health Assessment Questionnaire (HAQ)/Childhood Health Assessment Questionnaire (C-HAQ), Childhood Myositis Assessment Scale (CMAS), Myositis Disease Activity Assessment Tool (MDAAT), Disease Activity Score (DAS), Short Form 36 (SF-36), Child Health Questionnaire (CHQ), physician global damage, Myositis Damage Index (MDI), Quantitative Muscle Testing (QMT), Myositis Functional Index-2 (FI-2), Myositis Activities Profile (MAP), Inclusion Body Myositis Functional Rating Scale (IBMFRS), Cutaneous Dermatomyositis Disease Area and Severity Index (CDASI), Cutaneous Assessment Tool (CAT), Dermatomyositis Skin Severity Index (DSSI), Skindex, and Dermatology Life Quality Index (DLQI). Arthritis Care Res. 2011;63 Suppl 11:S118–57.

32. Mammen AL. Autoimmune myopathies: autoantibodies, phenotypes and pathogenesis. Nat Rev Rheumatol. 2011;7:343–54.

33. Vencovsky J, Jarosova K, Machacek S, et al. Cyclosporine A versus methotrexate in the treatment of polymyositis and dermatomyositis. Scand J Rheumatol. 2000;29:95–102.

34. Dastmalchi M, Grundtman C, Alexanderson H, et al. A high incidence of disease flares in an open pilot study of infliximab in patients with refractory inflammatory myopathies. Ann Rheum Dis. 2008;67:1670–7.

35. Rider LG, Lachenbruch PA, Monroe JB, et al. Damage extent and predictors in adult and juvenile dermatomyositis and polymyositis as determined with the myositis damage index. Arthritis Rheum. 2009;60:3425–35.

36. Allanore Y, Vignaux O, Arnaud L, et al. Effects of corticosteroids and immunosuppressors on idiopathic inflammatory myopathy related myocarditis evaluated by magnetic resonance imaging. Ann Rheum Dis. 2006;65:249–52.

37. Danko K, Ponyi A, Constantin T, et al. Long-term survival of patients with idiopathic inflammatory

myopathies according to clinical features: a longitudinal study of 162 cases. Medicine (Baltimore). 2004;83:35–42.

38. Friedrich MG, Sechtem U, Schulz-Menger J, et al. Cardiovascular magnetic resonance in myocarditis: a JACC White Paper. J Am Coll Cardiol. 2009;53:1475–87.

39. Samson C, Soulen RL, Gursel E. Milk of calcium fluid collections in juvenile dermatomyositis: MR characteristics. Pediatr Radiol. 2000;30:28–9.

40. Partovi S, Schulte AC, Aschwanden M, et al. Impaired skeletal muscle microcirculation in systemic sclerosis. Arthritis Res Ther. 2012;14:R209.

41. Park JH, Vital TL, Ryder NM, et al. Magnetic resonance imaging and P-31 magnetic resonance spectroscopy provide unique quantitative data useful in the longitudinal management of patients with dermatomyositis. Arthritis Rheum. 1994;37:736–46.

42. Cea G, Bendahan D, Manners D, et al. Reduced oxidative phosphorylation and proton efflux suggest reduced capillary blood supply in skeletal muscle of patients with dermatomyositis and polymyositis: a quantitative 31P-magnetic resonance spectroscopy and MRI study. Brain. 2002;125:1635–45.

43. Qi J, Olsen NJ, Price RR, et al. Diffusion-weighted imaging of inflammatory myopathies: polymyositis and dermatomyositis. J Magn Reson Imaging. 2008;27:212–7.

44. Maillard SM, Jones R, Owens C, et al. Quantitative assessment of MRI T2 relaxation time of thigh muscles in juvenile dermatomyositis. Rheumatology. 2004;43:603–8.

45. Maillard SM, Jones R, Owens CM, et al. Quantitative assessments of the effects of a single exercise session on muscles in juvenile dermatomyositis. Arthritis Rheum. 2005;53:558–64.

46. Parker L, Nazarian LN, Carrino JA, et al. Musculoskeletal imaging: medicare use, costs, and potential for cost substitution. J Am Coll Radiol. 2008;5:182–8.

47. Pillen S, Boon A, Van AN. Muscle ultrasound. Handb Clin Neurol. 2016;136:843–53.

48. Fornage BD. The case for ultrasound of muscles and tendons. Semin Musculoskelet Radiol. 2000;4:375–91.

49. Weber MA. Ultrasound in the inflammatory myopathies. Ann N Y Acad Sci. 2009;1154:159–70.

50. Reimers CD, Fleckenstein JL, Witt TN, et al. Muscular ultrasound in idiopathic inflammatory myopathies of adults. J Neurol Sci. 1993;116:82–92.

51. Batz R, Sofka CM, Adler RS, et al. Dermatomyositis and calcific myonecrosis in the leg: ultrasound as an aid in management. Skelet Radiol. 2006;35:113–6.

52. Brown AL, Murray JG, Robinson SP, et al. Case report: milk of calcium complicating juvenile dermatomyositis--imaging features. Clin Radiol. 1996;51:147–9.

53. Weber MA, Jappe U, Essig M, et al. Contrast-enhanced ultrasound in dermatomyositis- and polymyositis. J Neurol. 2006;253:1625–32.

54. Brudin LH, Valind SO, Rhodes CG, et al. Fluorine-18 deoxyglucose uptake in sarcoidosis measured with positron emission tomography. Eur J Nucl Med. 1994;21:297–305.

55. Hooisma GA, Balink H, Houtman PM, et al. Parameters related to a positive test result for FDG PET(/CT) for large vessel vasculitis: a multicenter retrospective study. Clin Rheumatol. 2012;31:861–71.

56. Owada T, Maezawa R, Kurasawa K, et al. Detection of inflammatory lesions by f-18 fluorodeoxyglucose positron emission tomography in patients with polymyositis and dermatomyositis. J Rheumatol. 2012;39:1659–65.

57. Pipitone N, Versari A, Zuccoli G, et al. 18F-Fluorodeoxyglucose positron emission tomography for the assessment of myositis: a case series. Clin Exp Rheumatol. 2012;30:570–3.

58. Tanaka S, Ikeda K, Uchiyama K, et al. [18F]FDG uptake in proximal muscles assessed by PET/CT reflects both global and local muscular inflammation and provides useful information in the management of patients with polymyositis/dermatomyositis. Rheumatology. 2013;52:1271–8.

59. Sigurgeirsson B, Lindelof B, Edhag O, et al. Risk of cancer in patients with dermatomyositis or polymyositis. A population-based study. N Engl J Med. 1992;326:363–7.

60. Selva-O'Callaghan A, Grau JM, Gamez-Cenzano C, et al. Conventional cancer screening versus PET/CT in dermatomyositis/polymyositis. Am J Med. 2010;123:558–62.

61. Spies SM, Swift TR, Brown M. Increased 99mTc-polyphosphate muscle uptake in a patient with polymyositis: case report. J Nucl Med. 1975;16:1125–7.

62. Steinfeld JR, Thorne NA, Kennedy TF. Positive 99mTc-pyrophosphate bone scan in polymyositis. Radiology. 1977;122:168.

63. Walker UA, Garve K, Brink I, et al. 99mTechnetium pyrophosphate scintigraphy in the detection of skeletal muscle disease. Clin Rheumatol. 2007;26:1119–22.

64. Mercuri E, Bushby K, Ricci E, et al. Muscle MRI findings in patients with limb girdle muscular dystrophy with calpain 3 deficiency (LGMD2A) and early contractures. Neuromuscul Disord. 2005;15:164–71.

65. Tasca G, Iannaccone E, Monforte M, et al. Muscle MRI in Becker muscular dystrophy. Neuromuscul Disord. 2012;22 Suppl 2:S100–6.

66. Peters SA, Kley R, Tegenthoff M, et al. MRI in lipid-lowering agent-associated myopathy: a retrospective review of 21 cases. AJR Am J Roentgenol. 2010;194:W323–8.

67. Infection C-CNF, conditions m. Infectious myositis. Best Pract Res Clin Rheumatol. 2006;20:1083–97.

68. Soler R, Rodriguez E, Aguilera C, et al. Magnetic resonance imaging of pyomyositis in 43 cases. Eur J Radiol. 2000;35:59–64.

69. Schwartz DM, Morgan ER. Multimodality imaging of Candida tropicalis myositis. Pediatr Radiol. 2008;38:473–6.

70. Jankharia BG, Chavhan GB, Krishnan P, et al. MRI and ultrasound in solitary muscular and soft tissue cysticercosis. Skelet Radiol. 2005;34:722–6.

71. Illa I, Nath A, Dalakas M. Immunocytochemical and virological characteristics of HIV-associated inflammatory myopathies: similarities with seronegative polymyositis. Ann Neurol. 1991;29:474–81.

72. Steinbach LS, Tehranzadeh J, Fleckenstein JL, et al. Human immunodeficiency virus infection: musculoskeletal manifestations. Radiology. 1993;186:833–8.

73. Dalakas MC, Pezeshkpour GH, Gravell M, et al. Polymyositis associated with AIDS retrovirus. JAMA. 1986;256:2381–3.

74. Fleckenstein JL, Burns DK, Murphy FK, et al. Differential diagnosis of bacterial myositis in AIDS: evaluation with MR imaging. Radiology. 1991; 179:653–8.

75. Khoury NJ, el-Khoury GY, Kathol MH. MRI diagnosis of diabetic muscle infarction: report of two cases. Skelet Radiol. 1997;26:122–7.

76. Jelinek JS, Murphey MD, Aboulafia AJ, et al. Muscle infarction in patients with diabetes mellitus: MR imaging findings. Radiology. 1999;211:241–7.

77. Lamminen AE, Hekali PE, Tiula E, et al. Acute rhabdomyolysis: evaluation with magnetic resonance imaging compared with computed tomography and ultrasonography. Br J Radiol. 1989;62:326–30.

78. Moratalla MB, Braun P, Fornas GM. Importance of MRI in the diagnosis and treatment of rhabdomyolysis. Eur J Radiol. 2008;65:311–5.

79. Silverstein A, Siltzbach LE. Muscle involvement in sarcoidosis, asymptomatic myositis, and myopathy. Arch Neurol. 1969;21:235–41.

80. Liem IH, Drent M, Antevska E, et al. Intense muscle uptake of gallium-67 in a patient with sarcoidosis. J Nucl Med. 1998;39:1605–7.

81. Otake S, Ishigaki T. Muscular sarcoidosis. Semin Musculoskelet Radiol. 2001;5:167–70.

82. Otake S. Sarcoidosis involving skeletal muscle: imaging findings and relative value of imaging procedures. AJR Am J Roentgenol. 1994;162:369–75.

83. Otake S, Banno T, Ohba S, et al. Muscular sarcoidosis: findings at MR imaging. Radiology. 1990;176:145–8.

84. Madariaga MG. Polymyositis-like syndrome in hypothyroidism: review of cases reported over the past twenty-five years. Thyroid. 2002;12:331–6.

85. Nalini A, Govindaraju C, Kalra P, et al. Hoffmann's syndrome with unusually long duration: report on clinical, laboratory and muscle imaging findings in two cases. Ann Indian Acad Neurol. 2014;17:217–21.

86. Chung J, Ahn KS, Kang CH, et al. Hoffmann's disease: MR imaging of hypothyroid myopathy. Skelet Radiol. 2015;44:1701–4.

87. Diekman EF, van der Pol WL, Nievelstein RA, et al. Muscle MRI in patients with long-chain fatty acid oxidation disorders. J Inherit Metab Dis. 2014;37:405–13.